https://doi.org/10.5194/egusphere-2026-3315
Preprint. Discussion started: 19 June 2026

Lateral Transport Controls Particulate Organic Carbon Stocks and Fluxes in the Baltic Sea

Lucas Porz[1], Jan Kossack[1], David Pogorzelski[1,2], Wenyan Zhang[1]

[1]Institute of Coastal Systems, Helmholtz-Zentrum Hereon, Max-Planck-Strasse 1, 21502 Geesthacht, Germany
[2] Overfly GmbH, Pappelallee 78/79, 10437 Berlin

Correspondence to: Lucas Porz (lucas.porz@hereon.de)

Abstract. The sediments of the Baltic Sea represent a substantial regional carbon sink. Yet, detailed mapping of organic carbon (OC) content and stock in the Baltic Sea is lacking, and our understanding of the transport pathways of particulate OC (POC) in the water column is limited. Here, we generate high-resolution (500×500 m) maps of surface OC content from available data using a deep neural network. The results are combined with porosity and Holocene sediment thickness maps to derive OC stocks per maritime zone of each Baltic Sea country. The total surface (top 10 cm) OC stock is estimated to 1.29 ± 0.36 GtC and the spatially averaged surface stock to 3.14 ± 0.86 kgC m^{-2}. A process-based, 3D numerical model is then used to simulate fluxes of resuspended POC. The results imply that horizontal transport of resuspended POC, rather than in-situ biological production, is the key factor determining the flux and distribution of sediment OC. Net horizontal transport of resuspended POC across maritime boundaries reaches the order of 1 MtC yr^{-1}, with substantial interannual variability. These fluxes are in the same magnitude as the recent net OC accumulation rate, underscoring the importance of laterally derived, allochthonous carbon in sedimentary Blue Carbon habitats. Regional numerical modelling may be useful in addressing the issues of double counting and additionality in Blue Carbon accounting and management.

1. Introduction

Organic carbon (OC) burial in marine sediments represents a substantial carbon sink in the Earth system on climate-relevant timescales. Stocks and sequestration capacities of various Blue Carbon habitats have recently been explored (Koplin et al., 2025; Piñeiro-Juncal et al., 2026), as well as impacts of human

https://doi.org/10.5194/egusphere-2026-3315
Preprint. Discussion started: 19 June 2026

sediment disturbances and potential management options to protect and strengthen sedimentary carbon stocks and sequestration (Porz et al., 2024; Macreadie et al., 2026). While many studies tend to focus on nearshore, vegetated Blue Carbon ecosystems, namely seagrass meadows, macroalgal and mangrove forests, and salt marshes, unvegetated sedimentary depocenters have recently received increased attention due to their comparatively large sequestration and storage capacity related to their vaster spatial extent along with high OC densities and sedimentation rates (Luisetti et al., 2019; Diesing et al., 2025). Several studies have focused on the Northwestern European shelf, and especially on the North Sea, where various high-resolution sediment and carbon maps have been compiled (Wilson et al., 2018; Bockelmann et al., 2018; Diesing et al., 2021). Conversely, other marine regions with less data coverage have received less attention.

In this study, we estimate sediment OC stock and particulate OC (POC) fluxes in the Baltic Sea, an epicontinental, brackish shelf sea in the northeast of Europe (Figure 1). Due to its distinct bathymetric features and sheltered location, the Baltic Sea basins represent exceptional sediment depocenters with high organic carbon contents. Various carbon budgets for the Baltic Sea have been compiled (e.g., Thomas et al., 2010; Kuliński and Pempkowiak, 2011; Gustafsson et al., 2014; Scheffold and Hense, 2020). However, benthic OC stock remains a considerable uncertainty in such budgets; due to a lack of spatially resolved maps of OC content, dry bulk density, and stock, existing estimates relied on extrapolations based on few data points.

A related issue regards the quantification of lateral POC fluxes, being controlled primarily by resuspension from the seabed and subsequent transport by currents (Almroth-Rosell et al., 2011; Nilsson et al., 2021). An understanding and quantification of lateral carbon fluxes is essential for determining the role of allochthonous carbon and, thereby, for accurate carbon budgeting in Blue Carbon ecosystems (Xiao et al., 2022; James et al., 2024; Kristensen et al., 2025). Substantial lateral sediment and POC transport can be expected in the Baltic Sea, especially in connection with episodic intrusions of high-salinity water masses (Major Baltic Inflows; MBIs) from the North Sea (Gingele and Leipe, 2001; Porz et al., 2021), which induce considerable bottom currents as they propagate between sub-basins.

https://doi.org/10.5194/egusphere-2026-3315
Preprint. Discussion started: 19 June 2026

To fill this gap, we use a Machine Learning (ML) approach to compile detailed spatial maps of OC content in the Baltic Sea sediments. We then use these maps to initialize a process-based, 3D hydrodynamics and sediment transport model to simulate the lateral fluxes of recalcitrant POC in the Baltic Sea.

2. Data and methods

2.1 Organic carbon content and stock mapping

Three datasets of surface organic carbon content are combined: The MOSAIC database (Paradis et al., 2023; *N*=453), point measurement data of Leipe et al. (2011; *N*=1471) and from the SECOS project (downloaded from the Baltic Sea Atlas; www.io-warnemuende.de/baltic-sea-atlas, last accessed 11. Sept. 2025; *N*=817). These datasets partially overlap, resulting in a total of 2617 unique data points.

We use two methods for estimating OC content in the entre Baltic from this data: (1) Kriging using the same parameters as Leipe et al. (2011), and a Machine Learning (ML) method. For the latter, we apply a feed-forward Deep Neural Network with Monte-Carlo Dropout and three hidden layers. The following input features (predictor variables) are selected: longitude (in degrees), latitude (in degrees), water depth (in meters; BSHC, 2013), and distance from coast (in kilometers; OBPG, 2012). A random dropout rate of 20% between layers is chosen, and 100 instances of model training and evaluation are performed, each with different neurons turned off randomly. This method has been shown to enhance model robustness and reduce overfitting (Gal and Ghahramani, 2016).

The OC measurements data points (Figure 1) are distributed unevenly in space, with densely sampled areas such as the Arkona Basin and sparsely sampled regions such as the Bothnian Bay, which may lead to overtraining of the model in the densely sampled areas and reduced model accuracy in sparsely sampled areas. To counter this, spatial density weighting is applied, where training data are weighted inversely with the number of points within a defined radius.

To evaluate the performance of both methods, we split the data into a training (80%; *N*=2094) and a testing (20%; *N*=523) dataset (Figure 1). Due to the uneven distribution of data points in space, the testing data points are defined using Farthest Point Sampling (FPS), maximizing the distance between testing

https://doi.org/10.5194/egusphere-2026-3315
Preprint. Discussion started: 19 June 2026

data points, and ensuring maximum spatial coverage of testing data. To avoid areas without training data in the validation in sparsely sampled regions, we add the additional constraint that the data point closest to each test data point remains a training data point. This heuristic promotes a more balanced distribution of testing and training data compared to random point sampling or FPS alone, with the goal of making metrics for model validation more meaningful.

We perform a hyperparameter search with a total of 216 combinations of parameters to find the optimal training parameters, as defined by the lowest RMSE between the prediction and the testing dataset, yielding the following optimal parameters: number of artificial neurons in each hidden layer: [128, 64, 32]; dropout rate between layers: 10%; batch size: 32; model learning rate: 0.002; spatial weighting radius: 0.25°. Using these optimal parameters, 100 instances of OC prediction using the Monte-Carlo Dropout method described above are performed on the same 500 m × 500 m grid as the bathymetry data (BSHC, 2013) for the entire Baltic Sea.

In order to compute the Holocene OC stock, OC content is multiplied with Holocene sediment thickness provided by Miluch et al. (2025) and with dry bulk density (Figure 2). Surface OC stock is calculated in the same way but using a constant thickness of 10 cm. Dry bulk density is calculated from porosity maps assuming a grain density of 2650 g cm^{-3}. Porosity is computed from a grain size map (Bobertz et al., 2009) using the empirical relationship of Endler et al. (2015). Uncertainties in OC content and porosity are propagated in the calculation of stock. For OC content, spatially resolved uncertainty is considered through the standard deviations of all Monte-Carlo Dropout runs. For porosity, a constant uncertainty of 0.073 is used, which is the standard deviation between measured and calculated porosities in the empirical relationship of Endler et al. (2015). Stocks are generated for each maritime zone according to maritime boundaries (Flanders Marine Institute, 2023), which include the Exclusive Economic Zones (EEZ), archipelagic waters, internal waters, and territorial seas of each country. As Holocene thickness data is not available for the Kattegat and Belt Sea (see Figure 2a), those areas are not included in the calculation of total Holocene OC stock.

https://doi.org/10.5194/egusphere-2026-3315
Preprint. Discussion started: 19 June 2026

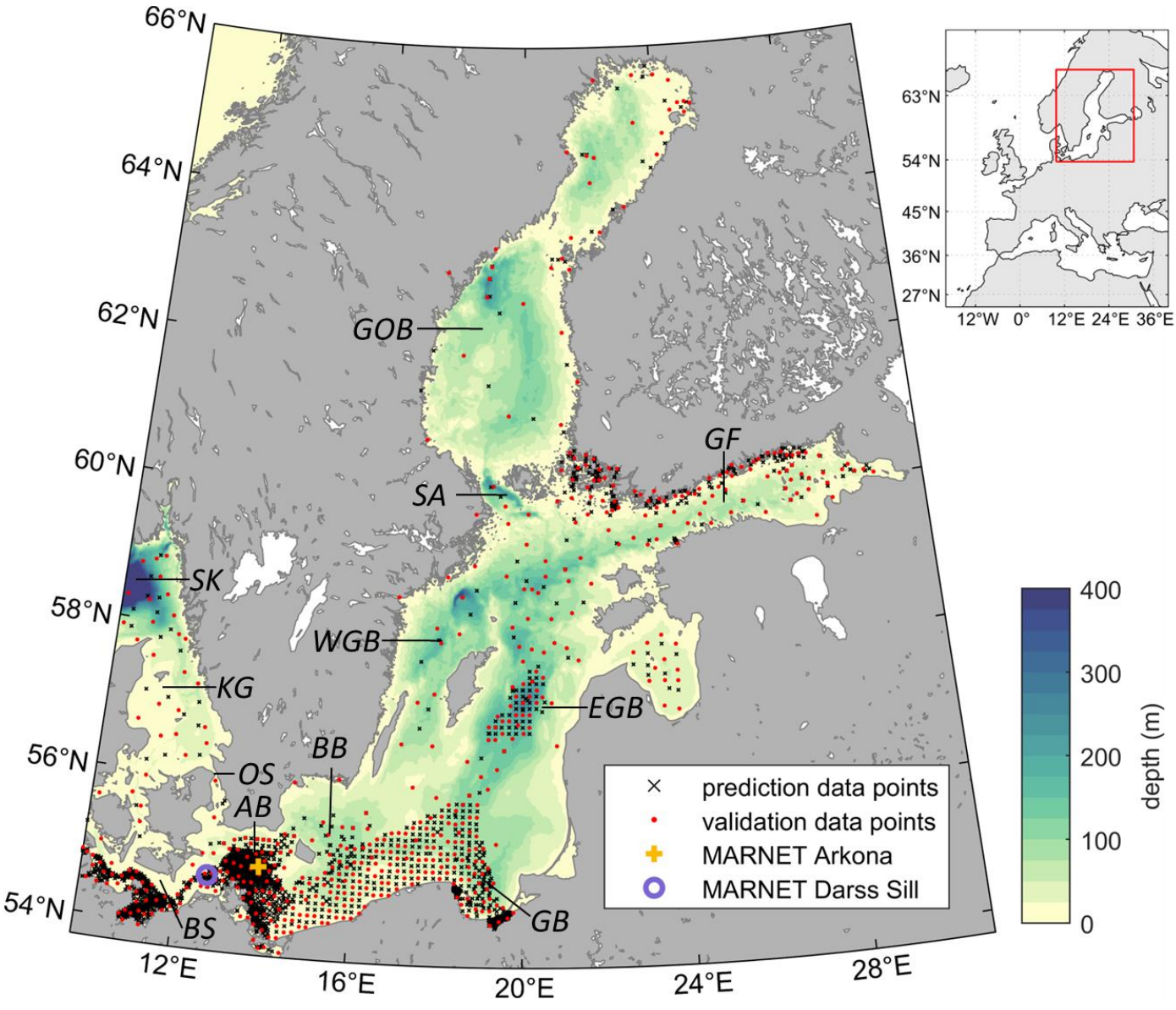

Figure 1. Baltic Sea study area with bathymetry and locations of available surface organic carbon content used as prediction data points (N=2094; black crosses) and validation (testing) data points (N=523; red dots) for mapping, as well as the MARNET monitoring stations used for validation of the hydrodynamic model. SK: Skagerrak, KG: Kattegat, OS: Sound, BS: Belt Sea, AB: Arkona Basin, BB: Bornholm Basin, GB: Gdansk Basin, WGB: Western Gotland Basin, EGB: Eastern Gotland Basin, SA: Sea of Åland, GOB: Gulf of Bothnia, GF: Gulf of Finland.

https://doi.org/10.5194/egusphere-2026-3315
Preprint. Discussion started: 19 June 2026

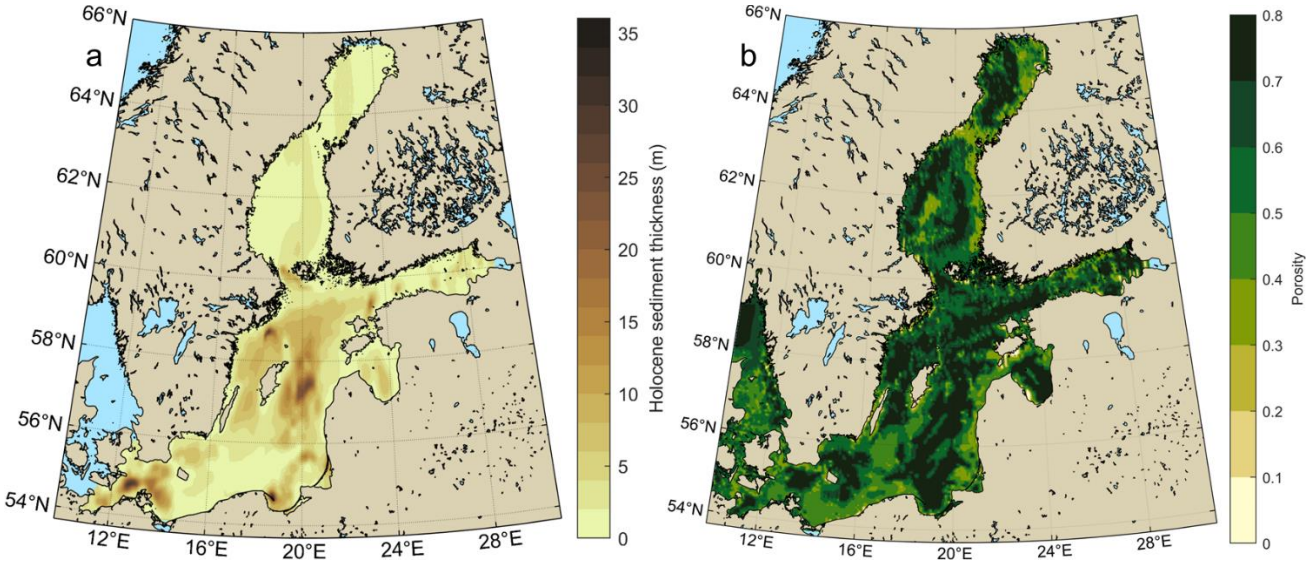

Figure 2. (a) Holocene sediment thickness and (b) porosity according to Miluch et al. (2025) used in the calculation of organic carbon stock.

2.2 Numerical model

The coupled numerical modelling system used in this study comprises the Semi-implicit Cross-scale Hydroscience Integrated System Model (SCHISM; Zhang et al., 2016) for hydrodynamics, and a sediment transport and morphodynamics model (MORSELFE, Pinto et al., 2012) based on the Community Sediment Transport Model (CSTM; Warner et al., 2008) for sediment dynamics. Turbulent mixing is calculated using the General Ocean Turbulence Model (GOTM; Umlauf and Burchard, 2003). For the simulation of sea ice, SCHISM is further coupled with the sea ice module Icepack (v1.3.4; Wang et al., 2024).

The hydrodynamic setup of SCHISM is based on that of Kossack et al. (2023). The model domain encompasses the entire Northwestern European Shelf, including the Baltic Sea and extending past the shelf break into the North Atlantic. The horizontal resolution of the unstructured computational grid increases from 15–20 km in the North Atlantic to ~10 km on the shelf. For this study, the base resolution of the unstructured computational grid is increased to a node distance of 2 km in the Baltic Sea. The grid

https://doi.org/10.5194/egusphere-2026-3315
Preprint. Discussion started: 19 June 2026

resolution in the Belt Sea and Sound is additionally refined up to a minimum node distance of 500 m to adequately resolve exchange between the North Sea and Baltic Sea. To improve inter-basin exchange within the Baltic Sea, higher resolutions of ~1 km are further employed in the Bornholm Strait connecting the Arkona and Bornholm Basins and in the Åland Sea. We apply the highly flexible hybrid Localized Sigma Coordinate with shaved cells (LSC²) in the vertical dimension. The vertical layers range from of 58 layers in the deep ocean to 2 layers in shallow regions. The minimum water depth is 10 m. The reader is referred to Kossack et al. (2023) for detailed hydrodynamic parameter settings.

The model is run for 6 years for the period 2010-2015. Boundary forcing for temperature and salinity (Boyer et al., 2018) as well as dynamic oceanic forcing for SSH and horizontal velocities (Lyard et al., 2021; Samuelsen et al., 2022) are identical to Kossack et al. (2023). Daily river discharge is provided from a regional river dataset compiled and used by Daewel and Schrum (2013) and further updated as described by Zhao et al. (2019). Differing from the configuration applied in Kossack et al. (2023), this study uses the hindcast simulation coastDat-5 (Geyer et al., 2026) for atmospheric forcing. Further, the sea ice module is used for the simulation of sea ice in the Baltic Sea. This setup further applies the $k-\epsilon$ turbulence scheme. Temperature and salinity arere initialized from reanalysis data (CMEMS, 2025) in the Baltic Sea, and from the World Ocean Atlas (Boyer et al., 2018) for the Northwestern European Shelf.

Extensive model validation for the Northwestern European Shelf is provided in Kossack et al. (2023). We additionally compare model outputs against the permanent monitoring stations of the MARNET monitoring network (BSH, 2020) in the Arkona Basin and at Darss Sill (see Figure 1 for locations) during the exceptionally strong MBI of winter 2014/2015. The model adequately reproduces both salt intrusion and horizontal current velocities (see Appendix B for details).

The initialization of seabed sediment in the model is restricted to the study area in the Baltic Sea, including the Kattegat. Four sediment classes are defined, three of which represent inorganic particles (sand, silt, and clay), and one of which represents recalcitrant OC. The inorganic sediment fractions are initialized by applying a scaling relationship between OC content, mud content and median grain size found by Leipe et al. (2011) using 185 sediment samples from the western Baltic Sea. The seabed is discretized

https://doi.org/10.5194/egusphere-2026-3315
Preprint. Discussion started: 19 June 2026

into 30 vertical layers with an initial thickness of 1 cm per layer. Sediment layer thicknesses and sediment fractions are adjusted dynamically based on resuspension, deposition and mixing during the simulation. Resuspension occurs when the bottom shear stress calculated in the hydrodynamic model exceeds a critical value. Resuspended sediment is treated as a sinking tracer and can be mixed, transported, and redeposited. Parameter settings for the sediment model are listed in Appendix A. We assume POC to behave similarly to silt-sized particles, as it is usually adsorbed to fine-grained sediment (silt and clay), and presence of OC typically causes the formation of relatively stable, low-density microflocs (e.g. Virto et al., 2008). Therefore, the sediment class representing OC is treated identically to the inorganic silt class regarding its sediment dynamic properties.

Horizontal fluxes across maritime boundaries are calculated at each timestep at model runtime as the sum of fluxes across all grid element sides which are closest to the respective maritime boundary. Positive and negative fluxes are tallied separately. In case two countries have multiple, disconnected maritime boundaries (such as Sweden and Denmark or Germany and Denmark), fluxes from all boundary sections are aggregated. A further boundary is defined at the border to the North Sea to track fluxes into and out of the Baltic Sea.

3. Results

3.1 Organic carbon content map

The ML method (Figure 3a; RMSE=1.75 wt%, R^2=0.664) achieves slightly more accurate predictions than the Kriging interpolation (Figure 3c; RMSE=1.81 wt%, R^2=0.656) when evaluated at the testing points. The Kriging interpolation shows a similar pattern as the original map by Leipe et al. (2011), with the smooth and oscillatory patterns (Figure 3c), though a few areas show differences due to the increased number of observations compared to Leipe et al. (2011). Meanwhile, the ML method provides a much more detailed and finer-scale distribution pattern (Figure 3a). The two methods produce markedly different OC distributions, with differences in organic carbon content exceeding 5 wt% in some areas, such as the Eastern Gotland Basin (Figure 3d). According to the ML model, the average surface carbon

https://doi.org/10.5194/egusphere-2026-3315
Preprint. Discussion started: 19 June 2026

content of Baltic Sea sediments is 3.06 ± 0.51 wt%, while the Kriging interpolation produces a mean of 3.48 wt%.

The Monte-Carlo dropout technique provides a sense of model uncertainty through the standard deviations across the model runs (Figure 3b). The absolute uncertainty is highest in areas of high OC content such as the Eastern and Western Gotland Basins, while high relative uncertainty occurs in sparsely sampled areas such as the Gulf of Bothnia.

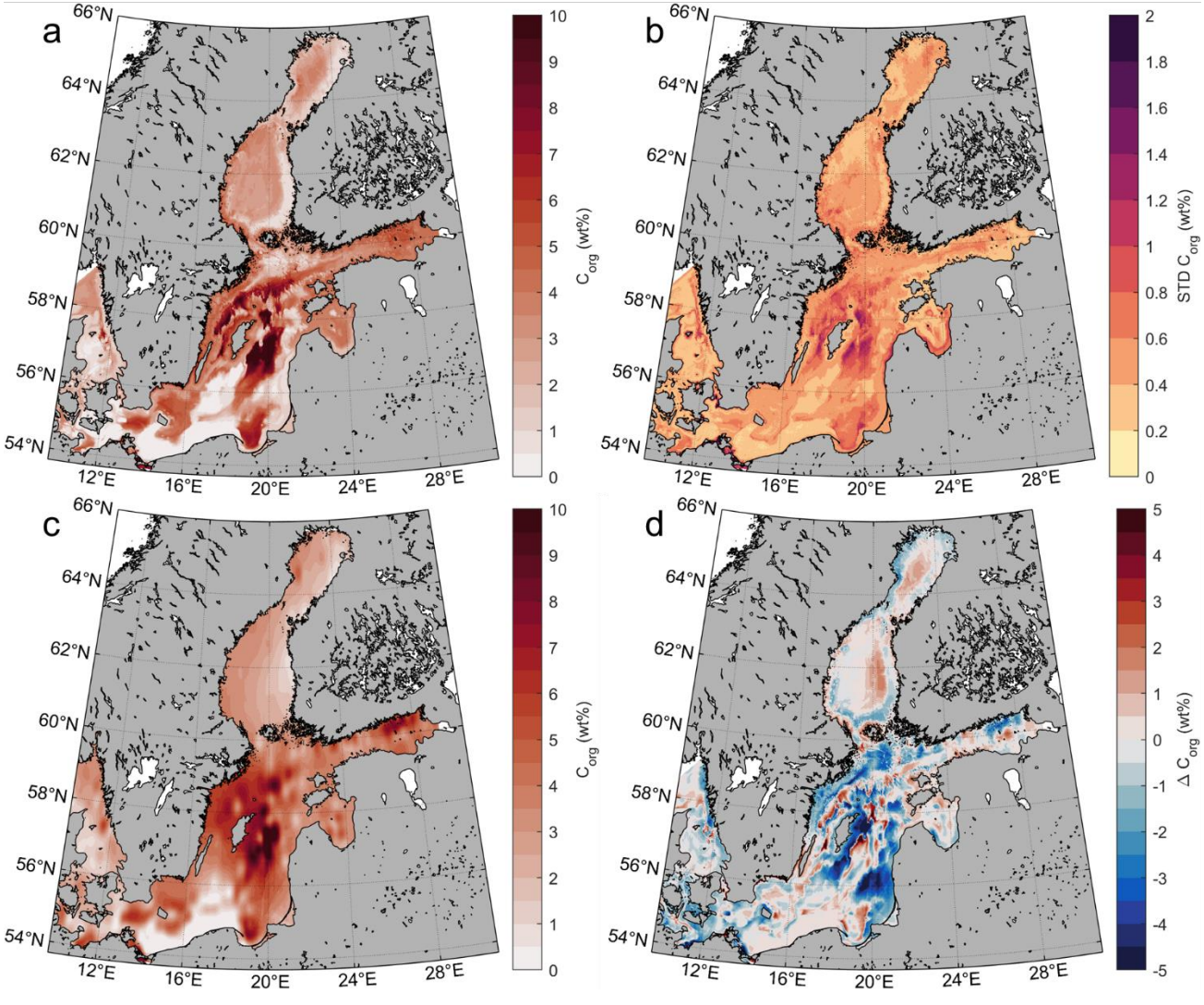

https://doi.org/10.5194/egusphere-2026-3315
Preprint. Discussion started: 19 June 2026

Figure 3. Surface organic carbon content in percent dry weight based on (a) the deep learning algorithm using optimal parameter set using the mean estimate of all Monte-Carlo runs, (b) standard deviation of estimated surface organic carbon contents of all Monte-Carlo runs, (c) Kriging interpolation performed using the same parameters as described in Leipe et al. (2011): nested variogram model using a nugget effect with an error of 1.5, a Gaussian model with a scale of 4 and a length of 25 km, and a Gaussian model with a scale of 8 and a length of 250 km, and (d) difference between (a) and (c).

3.2 Organic carbon stock

The surface OC stock in the top 10 cm sediments of the Baltic Sea is estimated to 1.29 ± 0.36 GtC. The spatially averaged surface OC stock amounts to 3.14 ± 0.86 kgC m^{-2}. Assuming vertical homogeneity of the Holocene sediment throughout its entire thickness, the total Holocene sediment OC stock (without Kattegat and Belt Sea) is 50.42 ± 14.10 GtC and the corresponding average stock is 132.10 ± 36.86 kgC m^{-2}. Relative uncertainty in these numbers is about 28% of the estimated values, with the uncertainty in OC content and porosity contributing about two thirds and one third to the total stock uncertainty, respectively.

Average OC content is overall comparable between maritime zones (Figure 4b), with the exceptions of Lithuania, Poland, and Germany, which have high proportions of shallow, sandy, and thus OC-poor areas. The maritime zone of Finland also has below-average OC content, likely tied to lower primary production in the Northern Baltic Sea. Sweden has the largest surface stock by far due to the vast extent of its maritime zone (Figure 4c), including large parts of the East Gotland Basin, which is the Baltic Sea's main Holocene OC depocenter. Average surface stock per area (Figure 4d) shows a slightly different pattern than OC content due to the effect of porosity. For example, the maritime zone of Denmark has relatively high average OC content, but relatively low average surface stock, since its main depocenter in the Bornholm Basin features high porosity and thus low bulk density.

Considering the entire Holocene thickness highlights the role of carbon depocenters (Figure 5), with the Eastern Gotland Basin as the main Holocene depocenter, and other, minor depocenters such as the Arkona, Bornholm, Western Gotland, and Gdansk Basins (Figure 5a). The average stock per maritime zone (Figure 5b) shows a markedly different pattern compared to that of the top meter (Figure 4d). For example, the estimated average Holocene stocks of the Finnish and Russian maritime zones are lower

https://doi.org/10.5194/egusphere-2026-3315
Preprint. Discussion started: 19 June 2026

compared to their top 10 cm stocks since although those zones contain areas rich in surface OC, they have overall low Holocene sediment thickness. Note that the average Holocene stocks of the Danish and Swedish maritime zones are not directly comparable to their surface stocks due to the lack of Holocene thickness data in the Kattegat and Belt Sea (see Figure 2a).

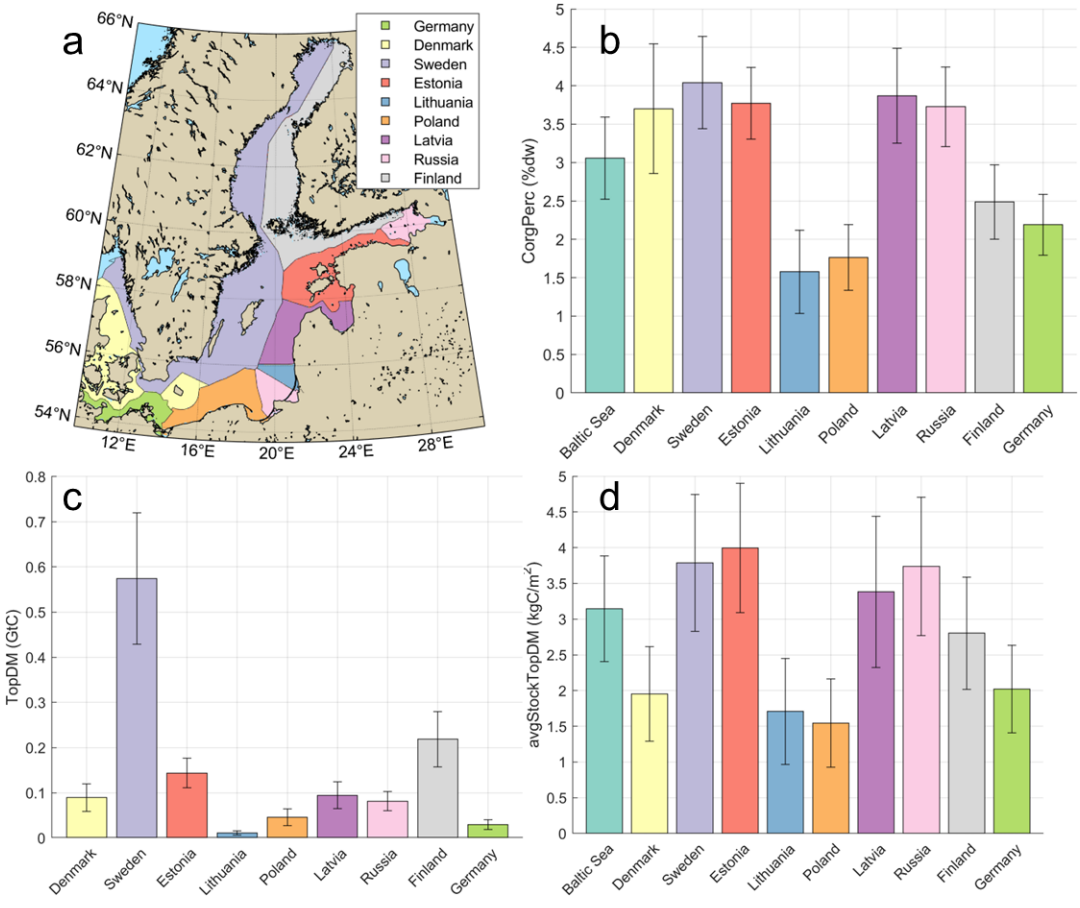

Figure 4. Sediment organic carbon inventory per maritime zone. (a) Maritime zones of all Baltic Sea countries, comprising their Exclusive Economic Zones, archipelagic waters, internal waters and territorial seas according to Flanders Marine Institute (2023). (b) Average surface sediment organic carbon content in percent dry weight based on the mapped data shown in Figure 3a. (c) Total surface organic carbon stock in (top 10 cm). (d) Average surface organic carbon stock (top 10 cm), calculated as total stock over total maritime area. Whiskers represent standard deviations arising from uncertainty in mapped carbon content and porosity.

https://doi.org/10.5194/egusphere-2026-3315
Preprint. Discussion started: 19 June 2026

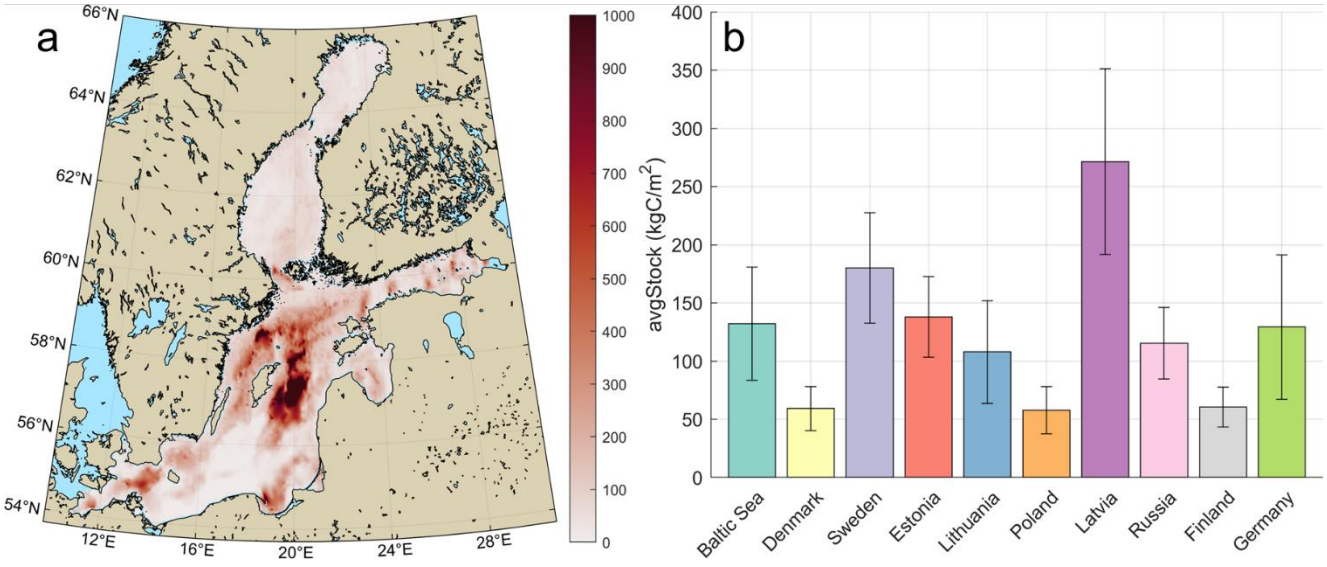

Figure 5. Holocene organic carbon stock in the Baltic Sea (without Kattegat and Belt Sea), assuming no variation of organic carbon content with depth in the sediment, shown as (a) a spatial map and (b) average stock per area for each maritime zone. Whiskers represent standard deviations arising from uncertainty in mapped carbon content and porosity.

3.3 Lateral organic carbon fluxes

Simulated lateral POC fluxes in the Baltic Sea range from less than 0.1 tC m^{-1} yr^{-1} in sandy, OC-poor areas such as the shallower areas at the Polish and Lithuanian coasts, to more than 100 tC m^{-1} yr^{-1} in the muddy, OC-rich Skagerrak and in the Belt Sea (Figure 6). Flux directions generally follow the bottom water circulation patterns of the Baltic, passing from the North Sea through the Kattegat and Belt Sea and eastward and northward across the basin-connecting sills. The signature of a cyclonic gyre is visible in the Eastern Gotland Basin, in line with a bottom stable circulation pattern expected in that area (Lehmann and Hinrichsen, 2000).

Interannual variability of simulated fluxes per maritime zones is substantial (Figure 7). In some cases, net transport switches between importing and exporting conditions, such as in the maritime zones of Finland, Poland, and Sweden. The German maritime zone switches from importing to exporting conditions from the simulation year 2012.

https://doi.org/10.5194/egusphere-2026-3315
Preprint. Discussion started: 19 June 2026

Fluxes of POC across maritime zone boundaries are considerably larger than the net fluxes (Figure 8), in most cases by an order of magnitude, highlighting the large spatiotemporal variability. For example, POC import to the German maritime zone from the Danish maritime zone (1305 ktC yr^{-1}) is nearly cancelled by an opposing POC export (1278 ktC yr^{-1}), leaving a net import of only 27 ktC yr^{-1}. Largest POC fluxes occur between the maritime zones of Demark and Sweden due to the great length of their shared border. Significant import of 660 ± 438 ktC yr^{-1} also occurs from the North Sea to the Baltic Sea.

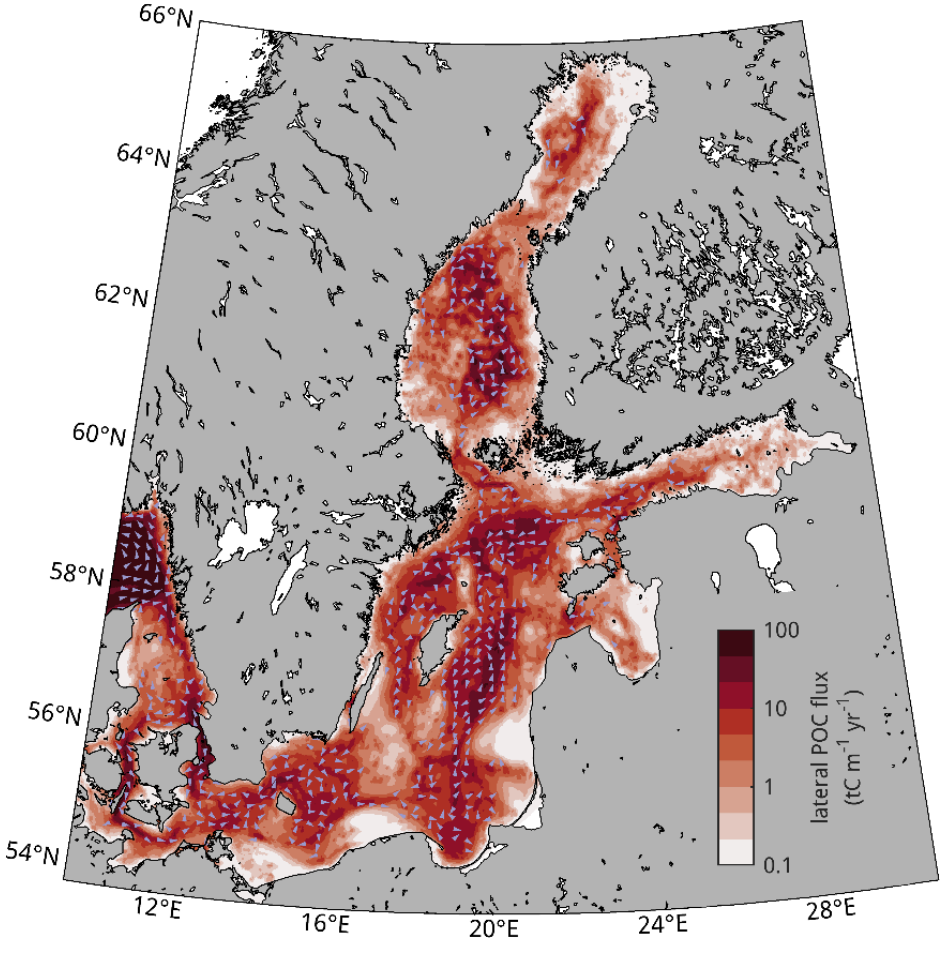

Figure 6. Lateral fluxes of resuspended particulate organic carbon in the Baltic Sea. Colours and arrows show magnitudes and arrows show directions of the residual, depth-integrated fluxes during the simulation period 2010–2015. Values are interpolated to regular grids for presentation. Arrows are shown only where the flux exceeds 1 tC m^{-1} yr^{-1}.

https://doi.org/10.5194/egusphere-2026-3315
Preprint. Discussion started: 19 June 2026

255

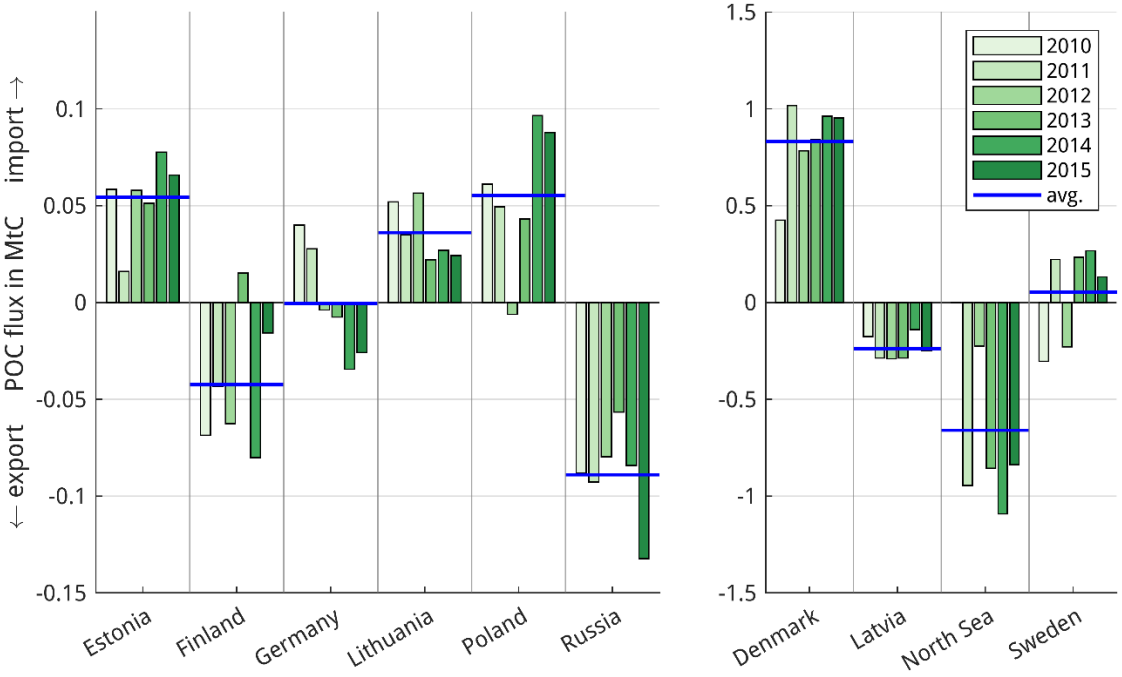

Figure 7. Lateral fluxes of particulate organic carbon per maritime zone and year. Net flux after each simulation year, where negative and positive values denote net flux out of and into the maritime zone, respectively. Blue lines indicate averages over the entire simulation period. Maritime zones are separated into two groups with different axis limits for better visual representation.

260

https://doi.org/10.5194/egusphere-2026-3315
Preprint. Discussion started: 19 June 2026

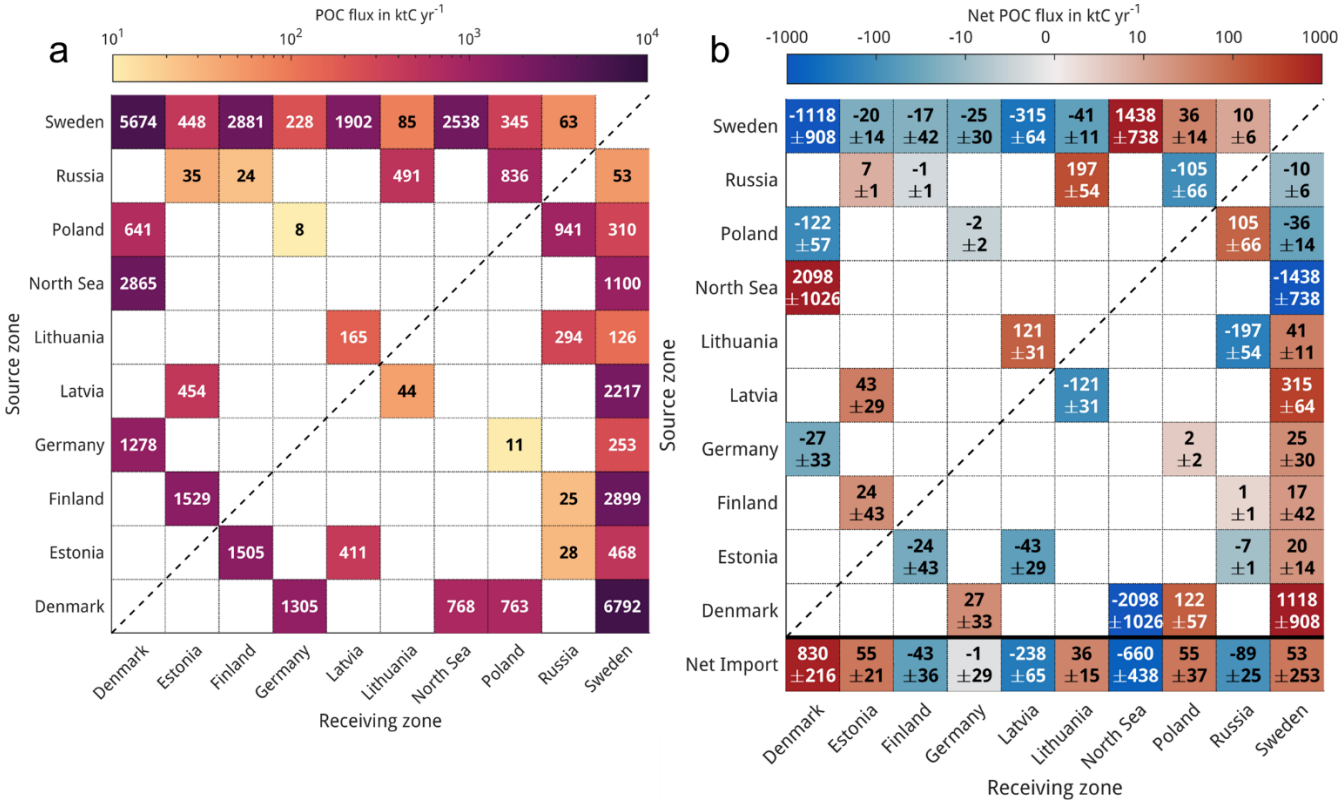

Figure 8. Lateral fluxes between maritime zones. Mean annual fluxes are shown for the six-year simulation period 2010–2015 with (a) flux from source (y-axis) to receiving (x-axis) maritime zone, where fluxes into and out of each maritime zone are tallied separately, and (b) mean net flux and standard deviation across years calculated as difference of fluxes into and out of each maritime zone, with the last row indicating net import (positive values) or net export (negative values).

4. Discussion

4.1 Comparison to existing stock estimates

The average OC content of 3.06 ± 0.51% dry weight compares well against the value of 3.03% found in Parameswaran et al. (2025). That study also used a neural network approach but included global datasets of 139 features such as seafloor lithologies, benthic oxygen fluxes, and chlorophyll-a satellite data. By contrast, our method produces a similar result using only four features (latitude, longitude, depth, and distance from coast), implying that a limited number of relevant features may suffice to produce reliable regional seafloor OC maps. A greater number of features requires more involved data acquisition, pre-

https://doi.org/10.5194/egusphere-2026-3315
Preprint. Discussion started: 19 June 2026

processing, and computational demand. In addition, many features, such as bottom current strength, are not based on direct measurements, but on outputs from hydrodynamic numerical ocean models. Hydrodynamic models themselves rely on several predefined inputs, some of which may be poorly constrained, such as bottom roughness length. Thereby, features extracted from such model outputs may introduce artificial biases in predicted fields of an ML model.

Parameswaran et al. (2025) estimate the total OC stock in the top 10 cm in the Baltic Sea to 0.77 GtC, considerably smaller than the 1.29 ± 0.36 GtC found in this study. The difference is likely explained by different assumptions on porosity and dry bulk density. Parameswaran et al. (2025) applied a global porosity map by Martin et al. (2015) derived using an ML approach, while our porosity map uses regional sediment properties and empirical scaling relationships to estimate porosity. This indicates that porosity (and dry bulk density) are key considerations in accurate OC stock mapping, as recently highlighted by Chatting et al. (2025).

Our estimated average OC stock in the top 10 cm of 3.14 ± 0.86 kgC m^{-2} is also significantly larger than the 0.83 ± 0.09 kgC m^{-2} of Scheffold and Hense (2020) which was estimated based on an extrapolation of 42 data points.

4.2 Holocene organic carbon accumulation rates

A tentative average Holocene OC burial rate can be derived by dividing the total stock by the time since the transition of the Baltic Sea from the glacial meltwater Baltic Ice Lake stage to the brackish Yoldia Sea stage, coinciding roughly with the onset of the Holocene around 11.7 cal. kyr BP (Rosentau et al., 2021). This yields a long-term averaged OC sequestration for the Baltic Sea (without Kattegat and Belt Sea) of 4.3 ± 1.20 MtC yr^{-1}. However, geological studies show a sudden shift toward higher OC content that occurred during the Holocene at the Littorina transgression around 8 cal. kyr BP (Sohlenius et al., 1996; Andrén et al., 2000), after which sediment OC content and accumulation rates have remained remarkably stable. Sediment cores covering the entire Holocene suggest that Holocene sections deposited prior to the Littorina transgression are similar in thickness to those deposited since then (Sohlenius et al., 1996; Andrén et al., 2000), implying an overestimation of the Holocene OC stock by a factor of up to two

https://doi.org/10.5194/egusphere-2026-3315
Preprint. Discussion started: 19 June 2026

when using the entire Holocene thickness. Assuming that post-Littorina sediments account for half of the Holocene sediment thickness and a transgression age of 8 cal. kyr BP brings the total burial rate to 3.15 ± 0.88 MtC yr^{-1}. Limiting this to accumulation areas, estimated here as areas where Holocene sediment thickness is at least two meters, which is roughly equivalent to the extent of depocenters, yields a burial rate of 2.50 ± 0.71 MtC yr^{-1}.

All of the values computed above are in range of the value of 3.20 ± 2.62 MtC yr^{-1} computed by Leipe et al. (2011) for accumulation areas based on dated surface sediment cores. They are also in agreement with recent OC burial of 2.73 ± 1.12 MtC yr^{-1} estimated by Kuliński and Pempkowiak (2011), calculated as the difference between accumulation rates from dated cores and long-term benthic mineralization. On the other hand, these numbers are somewhat higher than burial rate estimates by Gustafsson et al. (2014; 1.9 ± 0.12 MtC yr^{-1}), Winogradow and Pempkowiak (2014; 1.96 ± 0.59 MtC yr^{-1}), and Nilsson et al. (2019; 0.98 ± 0.31 MtC yr^{-1}), indicating that OC burial in the Baltic is not yet fully understood. The reasons for these discrepancies are difficult to disentangle; aside from differences in methodology, the studies differ in terms of considered timescale, exact spatial extent, and consideration of spatial variability. Nevertheless, total post-Littorina OC accumulation rates in the range of 2–3 MtC yr^{-1} seem likely. Fully addressing this issue requires a compilation of basin-wide Littorina-stage thickness maps, ideally incorporating downcore variations in OC content and bulk density.

4.3 Importance of lateral fluxes

Our results illustrate that lateral fluxes of resuspended POC are in the same magnitude as sedimentation in depocenters. The important role of lateral transport is also highlighted by Struck et al. (2004), whose sediment traps in the Eastern Gotland Basin measured sedimentation rates two- to sevenfold higher than observed vertical settling fluxes, the difference being attributed to lateral transport. Nilsson et al. (2021) demonstrate using in-situ POC recycling measurements that lateral particle transport is an important process in all major basins of the Baltic Sea, transporting POC of different origins and reactivity toward depocenters. Similarly, Spiegel et al. (2025) show based on sediment cores and benthic lander measurements that lateral POC import governs accumulation and estimate the proportion of lateral POC

https://doi.org/10.5194/egusphere-2026-3315
Preprint. Discussion started: 19 June 2026

input to 82 ± 6% in the Skagerrak, which is the main sediment depocenter in the North Sea at the transition to the Baltic Sea.

Interestingly, the budget analysis by Thomas et al. (2010) and Kuliński and Pempkowiak (2011) suggest a net export of OC from the Baltic Sea to the North Sea of 0.6 and 1.67 ± 0.22 MtC yr^{-1}, respectively, while our model finds a net POC import of 0.66 MtC yr^{-1}. This discrepancy is likely explained by two related factors: Firstly, Thomas et al. (2010) and Kuliński and Pempkowiak (2011) do not consider depth-resolved transport, instead scaling OC flux with net water mass outflow toward the North Sea. The second reason is that their estimate mainly considers transport of dissolved OC, which is distributed more equally throughout the water column, whereas POC is mainly transported near the seafloor. Our results suggest that the export of dissolved OC to the North Sea is at least partly compensated by POC import near the seabed.

4.4 Implications for Blue Carbon budgeting

Our budgets show that the relative magnitudes of sediment OC stocks depend to a large degree on which metric is being compared; surface (top 10 cm) stock, area-averaged stock and total (Holocene) stock show different patterns when compared across maritime zones (Figure 4, Figure 5). Most Blue Carbon assessments to date are restricted to surface sediment, mainly due to the greater availability of surface OC content measurements. However, the focus on surface sediment is not justified from the perspective of carbon sequestration and budgeting, as surface OC must be considered in a transitional phase and typically contains more labile compounds of organic matter that do not contribute to carbon sequestration. This also leads to an underrepresentation of the contribution of depocenters, where porosities and burial rates are often highest. We argue that a constant time horizon is preferable over a constant depth interval when defining Blue Carbon stocks, which integrates spatial variability in burial rates and accounts for the effect of porosity. This is in line with a recent definition that requires carbon to be sequestered on climatically relevant timescales of at least 100 years to be considered Blue Carbon (ICES, 2024). This timescale matches a sediment thickness of 10 cm thickness only for sedimentation rates of 1 mm yr^{-1}, whereas areas with higher and lower rates would be under- and overrepresented, respectively. A similar argument was presented by Bradley et al. (2022) for the case of burial rates; those authors proposed quantifying

https://doi.org/10.5194/egusphere-2026-3315
Preprint. Discussion started: 19 June 2026

sedimentary OC sinks with sediment-depth and sediment-age-resolved metrics rather than through burial beyond an arbitrary reference depth. Our results support this notion and suggest it should be extended to the concept of carbon stocks as well.

Our simulated POC fluxes show high interannual variability, with even the direction of the net flux altering between import and export among the years, implying that reliable estimates of long-term net sequestration require averaging of longer (decadal or more) time-series. This also means that benefits arising from management measures aimed at strengthening Blue Carbon habitats may not become evident until decades after their establishment.

The issue of lateral fluxes is closely related to the open problems of additionality and double counting in Blue Carbon accounting, and it is currently debated whether and how allochthonous carbon should be considered in Blue Carbon ecosystems (Houston et al., 2024; Williamson et al., 2025; Houston et al., 2025). Proof of additionality, i.e., evidence of increased net carbon sequestration of an ecosystem, requires estimating the amount of carbon sequestration that would take place in the absence of that ecosystem, and this amount would be deducted from the Blue Carbon contribution. Further, it must be ensured that allochthonous carbon is not counted more than once when transported between areas. Existing laboratory methods used to quantify allochthonous carbon such as biomarkers and stable isotope analysis are deemed prohibitively complex or expensive (Houston et al., 2024). Numerical ocean models may be useful in resolving both issues, as they are mass-conservative and able to tally cross-boundary carbon fluxes. Combining and tuning of such models with measurement data may yield estimates sufficiently robust for inclusion in national greenhouse gas emission inventories, nationally determined contributions, and Blue Carbon markets.

4.5 Limitations

Although the ML method produces finer-scale spatial features in the OC content map compared to Kriging and despite both methods showing strong spatial differences, they perform similar in terms of validation metrics. This may be explained by the choice of testing data point distribution (FPS), which leaves only few training data points among the testing data points in scarcely sampled regions. Nevertheless, some

https://doi.org/10.5194/egusphere-2026-3315
Preprint. Discussion started: 19 June 2026

research suggests that though different mapping methods can generate results of similar quality, ML approaches tend to require less human intervention (Diesing et al., 2014). This also applies to our ML method, which requires little expert judgement in parameter selection. Although architecture and training parameters must be chosen, they can be identified by an automated hyperparameter search, whereas Kriging typically requires manual specification of a variogram model.

Though uncertainties in both OC content and porosity were considered, they apply mostly to surface values (top 10 cm). The true uncertainty of the total Holocene stock, in which variations in OC content or porosity with depth were not accounted for, may be considerably larger. The largest potential error stems from strong environmental shifts during the Early to Mid-Holocene. The Holocene OC stock of 50.42 ± 14.10 GtC may need to be discounted by up to 50% to account for the lower OC content of sediments preceding the Littorina transgression. The Littorina-stage variation of OC content found in cores of depositional basins can also reach around 20% of the average value (Sohlenius et al., 1996; Andrén et al., 2000). Miluch et al. (2025) further estimate neglection of the vertical compaction in these basins to an overestimation of the porosity by ~10 %, equivalent to an underestimation of stock by the same amount. Additionally, the unclear seismic boundary between Late Pleistocene and early Holocene sediment in the seismic profiles may cause relative errors in Holocene sediment thickness by about 20% (Miluch et al., 2025). A more reliable estimate of age-related stock will require compilation of basin-wide, Littorina-stage sediment thickness maps.

We consider only resuspension of stable POC from the existing seafloor in our simulations, ignoring any internal carbon cycling and creation of new POC through primary production. While ecosystem-targeted studies tend to feature the role of freshly produced organic matter and phyto-detritus from seasonal primary production as an important source of POC to the seafloor, this fraction is biochemically highly reactive and mostly respired within a year, whereas older, more stable forms of POC can be advected with currents over long distances through multiple cycles of resuspension, transport, and redeposition until ultimate burial. Nevertheless, transport of fresh POC in the water column is likely also considerable. Almroth-Rosell et al. (2011) show the relative importance of resuspended POC fluxes in the Baltic using

https://doi.org/10.5194/egusphere-2026-3315
Preprint. Discussion started: 19 June 2026

a biogeochemical model, where, depending on depth, 45–75% of sediment POC has been resuspended at least once, with a higher proportion of resuspended OC in shallower areas.

Another relevant source of OC not included in our study is riverine input. Kuliński and Pempkowiak (2011) estimate total OC discharge to the Baltic to 4.09 ± 0.77 MtC yr^{-1}, exceeding total burial. However, it is unclear how much of this OC is dissolved versus particulate, nor how much may be remineralized versus buried in sediments. This likely depends on the properties of the catchment from which OC in the soil is eroded, as well as on the biogeochemical processes within the rivers and estuaries. Based on lignin contents, Miltner and Emeis (2001) estimate a minor contribution of terrestrial OC to Baltic Sea sedimentation (10–30%), with the proportion decreasing with distance from the river source.

The numerical modelling system also includes limitations. While the hydrodynamics could be validated quantitatively, near-bottom data of POC or suspended sediment concentrations for validation of sediment dynamics is lacking in the study area. We therefore rely on literature values for estimating relevant sediment dynamic properties, namely critical shear stress, settling velocity, and erosion rate, but acknowledge that these have large uncertainties any of these may vary regionally. Nevertheless, previous studies using the same modelling framework and similar parameter settings showed some skill in reproducing near-bottom suspended sediment concentrations when compared against the few data points available (Porz et al., 2021), so we consider the magnitudes of transport rates to be overall reasonable.

5. Conclusions and Outlook

We present high-resolution (500 m × 500 m) maps of sediment OC content and stock for the Baltic Sea. The surface (top 10 cm) OC stock estimate of 1.29 ± 0.36 GtC is about six times greater than that of the North Sea (0.23 ± 0.13 GtC; Diesing et al., 2021), underscoring the Baltic Sea as an important regional carbon sink and reservoir. Aside from estimating carbon stocks, such high-resolution maps may be useful for upscaling measured benthic fluxes in space to derive more robust benthic flux estimates, for initializing biogeochemical models, or for gauging impacts of human disturbances on seafloor carbon storage. Lateral fluxes of resuspended POC are investigated using a 3D numerical coastal ocean model, finding that horizontal transport between maritime zones and its variability are of the same magnitude as

https://doi.org/10.5194/egusphere-2026-3315
Preprint. Discussion started: 19 June 2026

long-term sediment burial in those zones. Our results have several practical implications for Blue Carbon budgeting:

1. Sedimentary OC stocks are more meaningful when defined across horizons of constant time rather than constant depth,
2. Lateral POC import and export should be considered in carbon budgets of spatially confined areas (such as EEZs),
3. Measurable changes in OC accumulation rates may take decades to establish due to strong inter-annual variability in the magnitudes and directions of lateral fluxes,
4. Mass-conservative, spatially resolved, process-based models may be used to address challenges of additionality and double counting in Blue Carbon accounting.

Due to data limitations, we map OC stock for the entire Holocene, which can be considered too long a timespan to be applicable to modern and future Blue Carbon budgets. A challenge for future research is therefore mapping recent OC stock down to recent (<1 kyr) sedimentary layers, which requires integration of short sediment cores and/or shallow seismic data.

Though biogeochemical models aimed at resolving nutrient cycling often do not account for existing sediment OC of low lability, which is the main component of OC sequestration, the roles of primary production and the propagation of organic matter through the food web remain important considerations, as they control the assimilation of CO_2 and thereby to CO_2-drawdown from the atmosphere. The high computational cost of 3D models complicates estimates of uncertainty in the form of sensitivity analyses. Increasing model complexity, e.g. through inclusion of biogeochemical processes, will tend to increase computational cost and uncertainty further. For practical applications, reliable uncertainty estimates may be sought using models of reduced resolution and/or more limited spatial extent.

https://doi.org/10.5194/egusphere-2026-3315
Preprint. Discussion started: 19 June 2026

Appendix

A. Model parameter settings

Table A1. Sediment model parameter settings. For each fraction, set values are given for settling velocity (w_s), critical shear stress for resuspension (τ_c), and erosion rate (M_E; erosion formulation according to Winterwerp et al. (2012)).

	Clay	Silt	Sand	POC
w_s (mm s^{-1})	0.005	0.1	0.2	0.1
τ_c (Pa)	0.1	0.1	0.2	0.1
M_E (s m^{-1})	0.001	0.001	0.002	0.001

B. Hydrodynamic model validation

https://doi.org/10.5194/egusphere-2026-3315
Preprint. Discussion started: 19 June 2026

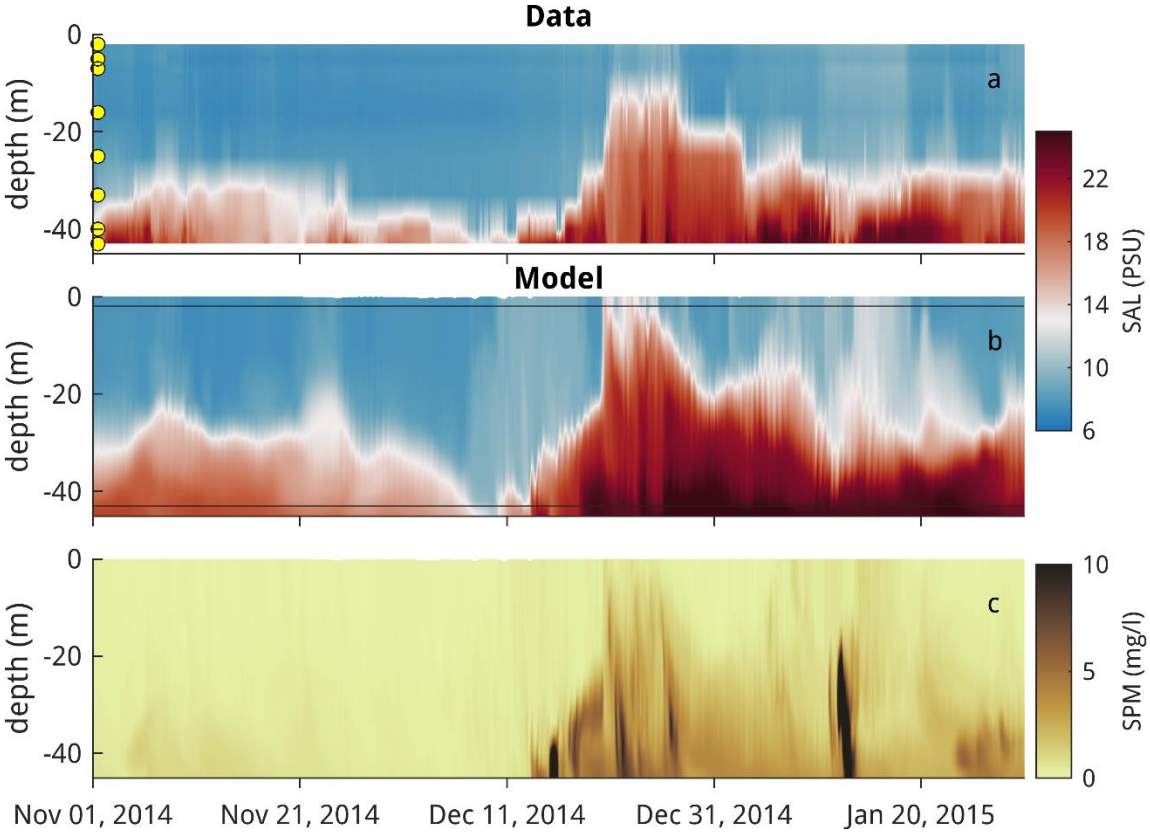

465 Figure A1. Time-series of (a) measured salinity, (b) modelled salinity, and (c) modelled suspended particulate matter concentration at the MARNET Arkona monitoring station located near the centre of the Arkona basin during the 2014/15 MBI. Yellow points in (a) denote the sensor depths, and horizontal lines in (b) denote the depth limits of the sensors for comparability.

https://doi.org/10.5194/egusphere-2026-3315
Preprint. Discussion started: 19 June 2026

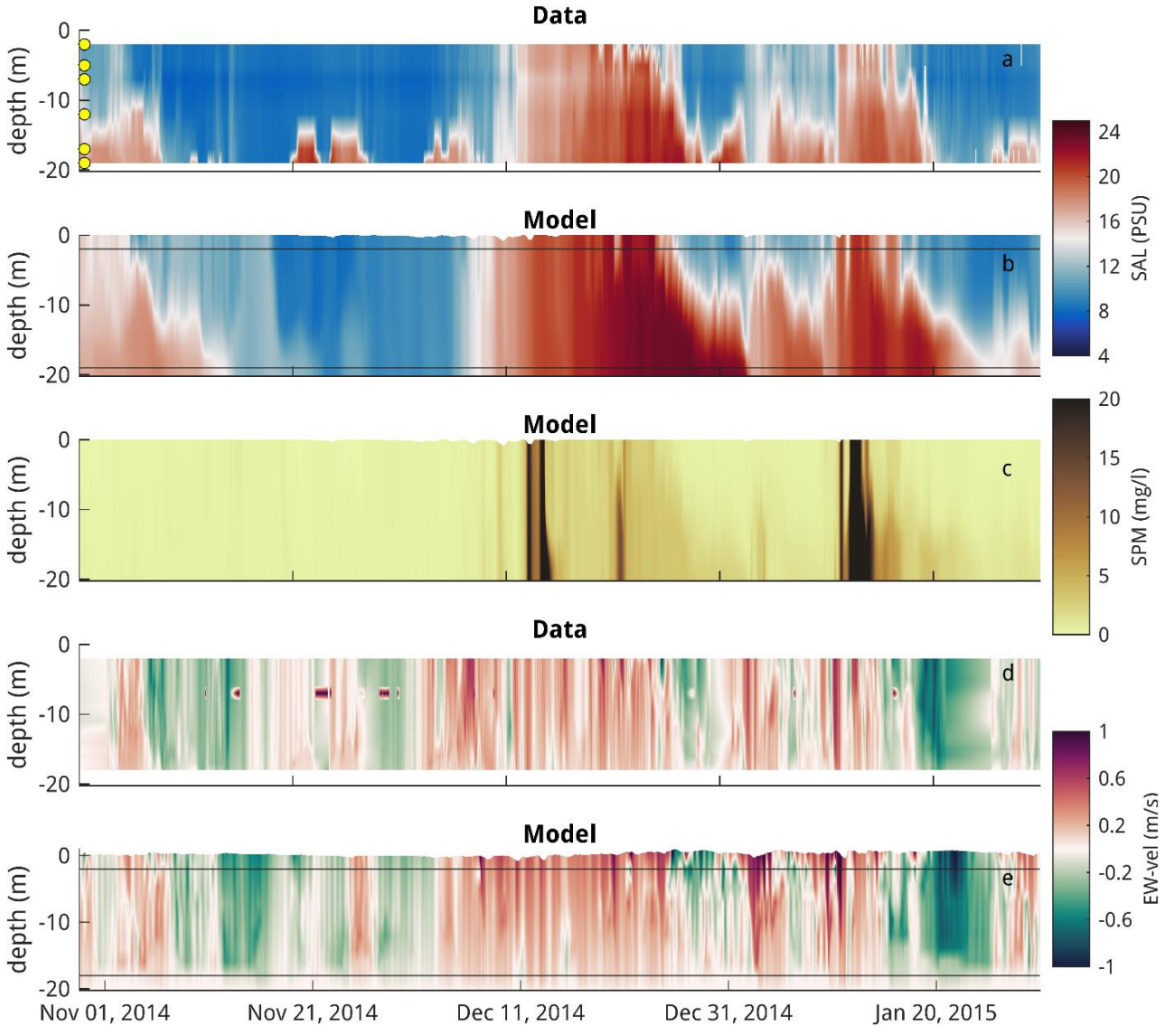

470 Figure A2. Time-series of (a) measured salinity, (b) modelled salinity, (c) modelled SPM concentration, (d) measured EW-current speed, and (e) modelled EW-current speed at the MARNET Darss Sill mooring station during the 2014/15 MBI. Yellow points in (a) denote sensor depths, and horizontal lines in (b,e) denote the respective depth limits of the sensors for comparability. Positive values in (d,e) denote eastward flow directions.

475

https://doi.org/10.5194/egusphere-2026-3315
Preprint. Discussion started: 19 June 2026

Code availability

The SCHISM model (v.5.11), including the sediment module MORSELFE and the sea ice module Icepack is available at https://github.com/schism-dev/schism/releases/tag/v5.11.0. The turbulence model GOTM (v.5.2) is available from https://github.com/gotm-model/code/tree/v5.2. Code modifications done for the purpose of this study are available upon request. Model parameter settings for SCHISM and code used in organic carbon content mapping will be uploaded to a permanent repository following manuscript acceptance.

Data availability

Organic carbon content and porosity maps will be uploaded to a permanent repository following manuscript acceptance. Holocene sediment thickness available at https://doi.org/10.17632/k45mff2ccy.1.

Author Contribution

LP and WZ conceptualized the study. LP designed the numerical model experiments and processed the outputs. JK developed the hydrodynamic numerical model setup. DP set up the machine learning model. LP drafted the manuscript in consultation with all co-authors.

Competing interest

The authors declare that they have no conflict of interest.

Acknowledgements

This work used resources of the German Climate Computing Centre (DKRZ) granted by its Scientific Steering Committee (WLA) under project IDs bg1244 and gg0877. The authors thank Thomas Leipe for providing measurement data of surface organic carbon content in the Baltic Sea. This study has been conducted using E.U. Copernicus Marine Service Information; https://doi.org/10.48670/moi-00013.

https://doi.org/10.5194/egusphere-2026-3315
Preprint. Discussion started: 19 June 2026

Financial support

This study is a contribution to the collaborative project KomSO (grant 3523NK370A-E) coordinated by the German Federal Agency for Nature Conservation (BfN). It is also supported by the Helmholtz research programme POF IV "The Changing Earth – Sustaining our Future" within "Topic 4: Coastal zones at a time of global change". J.K. was supported by the Deutsche Forschungsgemeinschaft (DFG, German Research Foundation) under Germany's Excellence Strategy – EXC 2037 'CLICCS - Climate, Climatic Change, and Society' – Project Number: 390683824 – CLICCS subproject A5 – The Land-Ocean Transition Zone. D.P. acknowledges the support by the Helmholtz Imaging Platform project "AutoCoast – Automatic detection of coastline change and causal linkage with natural and human drivers" (ZT-IPF-4-048).

Review statement

The review statement will be added by Copernicus Publications listing the handling editor as well as all contributing referees according to their status anonymous or identified.

References

Almroth-Rosell, E., Eilola, K., Hordoir, R., Meier, H. E. M., and Hall, P. O.: Transport of fresh and resuspended particulate organic material in the Baltic Sea — a model study, J. Mar. Sys., 87, 1–12, doi:10.1016/j.jmarsys.2011.02.005, 2011.

Andrén, E., Andrén, T., and Sohlenius, G.: The Holocene history of the southwestern Baltic Sea as reflected in a sediment core from the Bornholm Basin, Boreas, 29, 233–250, doi:10.1111/j.1502-3885.2000.tb00981.x, 2000.

Baltic Sea Hydrographic Commission (BSHC): Baltic Sea Bathymetry Database version 0.9.3.: http://data.bshc.pro/. 2013, last access: 20 April 2020.

Bobertz, B., Harff, J., and Bohling, B.: Parameterisation of clastic sediments including benthic structures, J. Mar. Sys., 75, 371–381, doi:10.1016/j.jmarsys.2007.06.010, 2009.

https://doi.org/10.5194/egusphere-2026-3315
Preprint. Discussion started: 19 June 2026

Bockelmann, F.-D., Puls, W., Kleeberg, U., Müller, D., and Emeis, K.-C.: Mapping mud content and median grain-size of North Sea sediments – A geostatistical approach, Mar. Geol., 397, 60–71, doi:10.1016/j.margeo.2017.11.003, 2018.

Boyer, T. P., García, H. E., Locarnini, R. A., Zweng, M. M., Mishonov, A. V., Reagan, J. R., Weathers, K. A., Baranova, O. K., Paver, C. R., and Seidov, D.: World Ocean Atlas 2018: https://www.ncei.noaa.gov/archive/accession/NCEI-WOA18. 2018, last access: 2022.

Bradley, J. A., Hülse, D., LaRowe, D. E., and Arndt, S.: Transfer efficiency of organic carbon in marine sediments, Nat. Comm., 13, 7297, doi:10.1038/s41467-022-35112-9, 2022.

Bundesamt für Seeschifffahrt und Hydrographie (BSH): Marine Environmental Monitoring Network in the North Sea and Baltic Sea: https://www.bsh.de/EN/TOPICS/Monitoring_systems/MARNET_monitoring_network/marnet_monitoring_network_node.html. 2020, last access: 11 November 2020.

Chatting, M., Diesing, M., Hunter, W. R., Grey, A., Kelleher, B. P., and Coughlan, M.: Improving marine sediment carbon stock estimates: the role of dry bulk density and predictor adjustments, Biogeosciences, 22, 5975–5990, doi:10.5194/bg-22-5975-2025, 2025.

Daewel, U. and Schrum, C.: Simulating long-term dynamics of the coupled North Sea and Baltic Sea ecosystem with ECOSMO II: Model description and validation, J. Mar. Sys., 119-120, 30–49, doi:10.1016/j.jmarsys.2013.03.008, 2013.

Diesing, M., Green, S. L., Stephens, D., Lark, R. M., Stewart, H. A., and Dove, D.: Mapping seabed sediments: Comparison of manual, geostatistical, object-based image analysis and machine learning approaches, Cont. Shelf Res., 84, 107–119, doi:10.1016/j.csr.2014.05.004, 2014.

Diesing, M., Sciberras, M., Thorsnes, T., Bjarnadóttir, L. R., and Moe, Ø. G.: Mapping organic carbon vulnerable to mobile bottom fishing in currently unfished areas of the Norwegian continental margin, Biogeosciences, 22, 7611–7624, doi:10.5194/bg-22-7611-2025, 2025.

Diesing, M., Thorsnes, T., and Bjarnadóttir, L. R.: Organic carbon densities and accumulation rates in surface sediments of the North Sea and Skagerrak, Biogeosciences, 18, 2139–2160, doi:10.5194/bg-18-2139-2021, 2021.

https://doi.org/10.5194/egusphere-2026-3315
Preprint. Discussion started: 19 June 2026

E.U. Copernicus Marine Service Information (CMEMS): Baltic Sea Physics Reanalysis: https://doi.org/10.48670/moi-00013. 2025, last access: 16 December 2025.

Endler, M., Endler, R., Bobertz, B., Leipe, T., and Arz, H. W.: Linkage between acoustic parameters and seabed sediment properties in the south-western Baltic Sea, Geo-Mar. Lett., 35, 145–160, doi:10.1007/s00367-015-0397-3, 2015.

Flanders Marine Institute: Maritime Boundaries Geodatabase: Maritime Boundaries and Exclusive Economic Zones (200NM), version 12: https://www.marineregions.org/. 2023.

Gal, Y. and Ghahramani, Z.: Dropout as a bayesian approximation: Representing model uncertainty in deep learning, Proceedings of The 33rd International Conference on Machine Learning, 48, 1050–1059, 2016.

Geyer, B., Campanale, A., Churiulin, E., Feldmann, H., Goergen, K., Hagemann, S., Ho-Hagemann, H. T. M., Karadan, M. M., Keuler, K., Khain, P., Lawand, D., Ludwig, P., Maurer, V., Petrov, S., Poll, S., Purr, C., Russo, E., Schubert-Frisius, M., Schulz, J.-P., Singh, S., Steger, C., Truhetz, H., and Will, A.: Optimisation of ICON-CLM for the EURO-CORDEX domain: developments, sensitivities, tuning, EGUsphere, 2026, 1–75, doi:10.5194/egusphere-2025-4726, 2026.

Gingele, F. X. and Leipe, T.: Southwestern Baltic Sea—A sink for suspended matter from the North Sea?, Geology, 29, 215, doi:10.1130/0091-7613(2001)029<0215:SBSASF>2.0.CO;2, 2001.

Gustafsson, E., Deutsch, B., Gustafsson, B. G., Humborg, C., and Mörth, C.-M.: Carbon cycling in the Baltic Sea — The fate of allochthonous organic carbon and its impact on air–sea CO2 exchange, J. Mar. Sys., 129, 289–302, doi:10.1016/j.jmarsys.2013.07.005, 2014.

Houston, A., Kennedy, H., and Austin, W. E. N.: Additionality in Blue Carbon Ecosystems: Recommendations for a Universally Applicable Accounting Methodology, Glob Change Biol, 30, e17559, doi:10.1111/gcb.17559, 2024.

Houston, A., Kennedy, H., and Austin, W. E. N.: Allochthonous Organic Carbon Stored in Blue Carbon Ecosystems Can Be Additional and Provide Genuine Climate Mitigation, Glob Change Biol, 31, e70182, doi:10.1111/gcb.70182, 2025.

ICES: Workshop on Assessing the Impact of Fishing on Oceanic Carbon (WKFISHCARBON; outputs from 2023 meeting), ICES Scientific Reports, 6, doi:10.17895/ices.pub.24949122.v1, 2024.

https://doi.org/10.5194/egusphere-2026-3315
Preprint. Discussion started: 19 June 2026

James, K., Macreadie, P. I., Burdett, H. L., Davies, I., and Kamenos, N. A.: It's time to broaden what we consider a 'blue carbon ecosystem', Glob Change Biol, 30, e17261, doi:10.1111/gcb.17261, 2024.

Koplin, J., Peter, C., Bischof, K., Böttcher, M. E., Kuhn, A., Logemann, E., Dolch, T., Henkel, S., McCarthy, D., Mueller, P., Morys, C., Pineda-Metz, S. E., Reents, S., Reusch, T. B., Röschel, L., Rupprecht, F., Stevenson, A., Wiltshire, K. H., Zimmer, M., and Pogoda, B.: Blue Carbon potential in Germany: Status and future development, Estuar. Coast. Shelf S., 323, 109354, doi:10.1016/j.ecss.2025.109354, 2025.

Kossack, J., Mathis, M., Daewel, U., Zhang, Y. J., and Schrum, C.: Barotropic and baroclinic tides increase primary production on the Northwest European Shelf, Front. Mar. Sci., 10, doi:10.3389/fmars.2023.1206062, 2023.

Kristensen, E., Flindt, M. R., and Quintana, C. O.: Predicting Climate Mitigation Through Carbon Burial in Blue Carbon Ecosystems—Challenges and Pitfalls, Glob Change Biol, 31, e70022, doi:10.1111/gcb.70022, 2025.

Kuliński, K. and Pempkowiak, J.: The carbon budget of the Baltic Sea, Biogeosciences, 8, 3219–3230, doi:10.5194/bg-8-3219-2011, 2011.

Lehmann, A. and Hinrichsen, H.-H.: On the wind driven and thermohaline circulation of the Baltic Sea, Physics and Chemistry of the Earth, Part B: Hydrology, Oceans and Atmosphere, 25, 183–189, doi:10.1016/S1464-1909(99)00140-9, 2000.

Leipe, T., Tauber, F., Vallius, H., Virtasalo, J. J., Uścinowicz, S., Kowalski, N., Hille, S., Lindgren, S., and Myllyvirta, T.: Particulate organic carbon (POC) in surface sediments of the Baltic Sea, Geo-Mar. Lett., 31, 175–188, doi:10.1007/s00367-010-0223-x, 2011.

Luisetti, T., Turner, R. K., Andrews, J. E., Jickells, T. D., Kröger, S., Diesing, M., Paltriguera, L., Johnson, M. T., Parker, E. R., Bakker, D. C., and Weston, K.: Quantifying and valuing carbon flows and stores in coastal and shelf ecosystems in the UK, Ecosystem Services, 35, 67–76, doi:10.1016/j.ecoser.2018.10.013, 2019.

Lyard, F. H., Allain, D. J., Cancet, M., Carrère, L., and Picot, N.: FES2014 global ocean tide atlas: design and performance, Ocean Sci, 17, 615–649, doi:10.5194/os-17-615-2021, 2021.

https://doi.org/10.5194/egusphere-2026-3315
Preprint. Discussion started: 19 June 2026

Macreadie, P. I., Biddulph, G. E., Masque, P., Kennedy, H., Samper-Villarreal, J., Patrick Megonigal, J., Morrissette, H. K., Romero-Gonzalez, T. E., Hatje, V., Friedrich, J., Sasmito, S. D., Watanabe, K., Mazarrasa, I., Krause-Jensen, D., Adams, J. B., Cifuentes-Jara, M., Arias-Ortiz, A., Rovai, A. S., Stankovic, M., Isensee, K., Queirós, A. M., Chen, L., Herrera-Silveira, J., Hurd, C. L., Ismail, R., Krauss, K. W., Lafratta, A., Palacios, M. M., and Austin, W. E. N.: Priority questions for the next decade of blue carbon science, Nature Ecology & Evolution, 10, 751–764, doi:10.1038/s41559-026-03020-6, 2026.

Martin, K. M., Wood, W. T., and Becker, J. J.: A global prediction of seafloor sediment porosity using machine learning, Geophys. Res. Lett., 42, 10,640-10,646, doi:10.1002/2015GL065279, 2015.

Miltner, A. and Emeis, K.-C.: Terrestrial organic matter in surface sediments of the Baltic Sea, Northwest Europe, as determined by CuO oxidation, Geochimica et Cosmochimica Acta, 65, 1285–1299, doi:10.1016/S0016-7037(00)00603-7, 2001.

Miluch, J., Zhang, W., Harff, J., Groh, A., Arlinghaus, P., and Denker, C.: Paleogeographic numerical modeling of marginal seas for the Holocene – an exemplary study of the Baltic Sea, Earth Syst. Dynam., 16, 585–605, doi:10.5194/esd-16-585-2025, 2025.

NASA Ocean Biology Processing Group (OBPG): Distance to the Nearest Coast: 0.01-Degree Grid: https://oceancolor.gsfc.nasa.gov/resources/docs/distfromcoast/. 2012, last access: 24 March 2025.

Nilsson, M. M., Hylén, A., Ekeroth, N., Kononets, M. Y., Viktorsson, L., Almroth-Rosell, E., Roos, P., Tengberg, A., and Hall, P. O.: Particle shuttling and oxidation capacity of sedimentary organic carbon on the Baltic Sea system scale, Marine Chemistry, 232, 103963, doi:10.1016/j.marchem.2021.103963, 2021.

Nilsson, M. M., Kononets, M., Ekeroth, N., Viktorsson, L., Hylén, A., Sommer, S., Pfannkuche, O., Almroth-Rosell, E., Atamanchuk, D., Andersson, J. H., Roos, P., Tengberg, A., and Hall, P. O.: Organic carbon recycling in Baltic Sea sediments – An integrated estimate on the system scale based on in situ measurements, Marine Chemistry, 209, 81–93, doi:10.1016/j.marchem.2018.11.004, 2019.

Paradis, S., Nakajima, K., van der Voort, T. S., Gies, H., Wildberger, A., Blattmann, T. M., Bröder, L., and Eglinton, T. I.: The Modern Ocean Sediment Archive and Inventory of Carbon (MOSAIC): version 2.0, Earth Syst. Sci. Data, 15, 4105–4125, doi:10.5194/essd-15-4105-2023, 2023.

https://doi.org/10.5194/egusphere-2026-3315
Preprint. Discussion started: 19 June 2026

Parameswaran, N., González, E., Burwicz-Galerne, E., Braack, M., and Wallmann, K.: NN-TOC v1: global prediction of total organic carbon in marine sediments using deep neural networks, Geosci. Model Dev., 18, 2521–2544, doi:10.5194/gmd-18-2521-2025, 2025.

Piñeiro-Juncal, N., Serrano, O., los Santos, C. B. de, Marbà, N., Díaz-Almela, E., Tuya, F., Mazarrasa, I., Garmendia, J. M., Otero, X. L., Inostroza, K., Pagès, J. F., Mendez-Martínez, G., Fernandez, E., Sousa, A. I., Camacho, A., Ballesteros, E., Barañano, C., Belshe, F., Bernabeu, I., Brun, F. G., Camacho-Santamans, A., Delgado, A., Dahl, M., Duarte, C. M., Espino, F., Franco, J., Da Conceiçao Freitas, M., Garcia-Orellana, J., Garrigos, B., Gomis, E., Haroun, R., Hernandez, I., Juanes, J. A., Leiva-Dueñas, C., Lavery, P., Lillebø, A. I., Lopes, V., Majtenyi-Hill, C., Marco-Mendez, C., Martins, M., Monnier, B., Morant, D., Montero, N., Neto, J. M., Ondiviela, B., Peralta, G., Picazo, A., Reithmaier, G., Rochera, C., Román, M., Santos, I. R., Santos, R., Serrano, E., Soler, M., Yau, Y. Y., Weitzmann, B., Zribi, I., and Mateo, M. Á.: Blue carbon inventories of Spain and Portugal for their inclusion in national climate mitigation strategies, Mar. Pollut. Bull., 228, 119570, doi:10.1016/j.marpolbul.2026.119570, 2026.

Pinto, L., Fortunato, A. B., Zhang, Y. J., Oliveira, A., and Sancho, F. E.: Development and validation of a three-dimensional morphodynamic modelling system for non-cohesive sediments, Ocean Model., 57, 1–14, doi:10.1016/j.ocemod.2012.08.005, 2012.

Porz, L., Zhang, W., Christiansen, N., Kossack, J., Daewel, U., and Schrum, C.: Quantification and mitigation of bottom-trawling impacts on sedimentary organic carbon stocks in the North Sea, Biogeosciences, 21, 2547–2570, doi:10.5194/bg-21-2547-2024, 2024.

Porz, L., Zhang, W., and Schrum, C.: Density-driven bottom currents control development of muddy basins in the southwestern Baltic Sea, Mar. Geol., 438, 106523, doi:10.1016/j.margeo.2021.106523, 2021.

Rosentau, A., Klemann, V., Bennike, O., Steffen, H., Wehr, J., Latinović, M., Bagge, M., Ojala, A., Berglund, M., Becher, G. P., Schoning, K., Hansson, A., Nielsen, L., Clemmensen, L. B., Hede, M. U., Kroon, A., Pejrup, M., Sander, L., Stattegger, K., Schwarzer, K., Lampe, R., Lampe, M., Uścinowicz, S., Bitinas, A., Grudzinska, I., Vassiljev, J., Nirgi, T., Kublitskiy, Y., and Subetto, D.:

https://doi.org/10.5194/egusphere-2026-3315
Preprint. Discussion started: 19 June 2026

A Holocene relative sea-level database for the Baltic Sea, Quaternary Science Reviews, 266, 107071, doi:10.1016/j.quascirev.2021.107071, 2021.

Samuelsen, A., Schrum, C., Yumruktepe, V. Ç., Daewel, U., and Roberts, E. M.: Environmental Change at Deep-Sea Sponge Habitats Over the Last Half Century: A Model Hindcast Study for the Age of Anthropogenic Climate Change, Front. Mar. Sci., 9, 737164, doi:10.3389/fmars.2022.737164, 2022.

Scheffold, M. I. E. and Hense, I.: Quantifying Contemporary Organic Carbon Stocks of the Baltic Sea Ecosystem, Front. Mar. Sci., 7, 2020.

Sohlenius, G., Sternbeck, J., Andrén, E., and Westman, P.: Holocene history of the Baltic Sea as recorded in a sediment core from the Gotland Deep, Mar. Geol., 134, 183–201, doi:10.1016/0025-3227(96)00047-3, 1996.

Spiegel, T., Dale, A. W., Lenz, N., Schmidt, M., Sommer, S., Becker, K. W., Elling, F. J., Porz, L., Daewel, U., Fuhr, M., Kalapurakkal, H. T., and Wallmann, K.: Benthic POC cycling in the Skagerrak basin: The role of lateral POC input, Cont. Shelf Res., 293, 105536, doi:10.1016/j.csr.2025.105536, 2025.

Struck, U., Pollehne, F., Bauerfeind, E., and v. Bodungen, B.: Sources of nitrogen for the vertical particle flux in the Gotland Sea (Baltic Proper)—results from sediment trap studies, J. Mar. Sys., 45, 91–101, doi:10.1016/j.jmarsys.2003.11.012, 2004.

Thomas, H., Pempkowiak, J., Wulff, F., and Nagel, K.: The Baltic Sea, in: Carbon and Nutrient Fluxes in Continental Margins: A Global Synthesis, Liu, K.-K., Atkinson, L., Quiñones, R., Talaue-McManus, L. (Eds.), Springer Berlin Heidelberg, Berlin, Heidelberg, 331–421, 2010.

Umlauf, L. and Burchard, H.: A generic length-scale equation for geophysical turbulence models, Journal of Marine Research, 61, 235–265, doi:10.1357/002224003322005087, 2003.

Virto, I., Barré, P., and Chenu, C.: Microaggregation and organic matter storage at the silt-size scale, Geoderma, 146, 326–335, doi:10.1016/j.geoderma.2008.05.021, 2008.

Wang, Q., Zhang, Y., Chai, F., Zhang, Y. J., and Zampieri, L.: Development of a total variation diminishing (TVD) sea ice transport scheme and its application in an ocean (SCHISM v5.11) and

https://doi.org/10.5194/egusphere-2026-3315
Preprint. Discussion started: 19 June 2026

sea ice (Icepack v1.3.4) coupled model on unstructured grids, Geosci. Model Dev., 17, 7067–7081, doi:10.5194/gmd-17-7067-2024, 2024.

Warner, J. C., Sherwood, C. R., Signell, R. P., Harris, C. K., and Arango, H. G.: Development of a three-dimensional, regional, coupled wave, current, and sediment-transport model, Computers & Geosciences, 34, 1284–1306, doi:10.1016/j.cageo.2008.02.012, 2008.

Williamson, P., Gore, C., Johannessen, S., Kristensen, E., Michaelowa, A., Wang, F., and Zhang, J.: Additionality Revisited for Blue Carbon Ecosystems: Ensuring Real Climate Mitigation, Glob Change Biol, 31, e70181, doi:10.1111/gcb.70181, 2025.

Wilson, R. J., Speirs, D. C., Sabatino, A., and Heath, M. R.: A synthetic map of the north-west European Shelf sedimentary environment for applications in marine science, Earth Syst. Sci. Data, 10, 109–130, doi:10.5194/essd-10-109-2018, 2018.

Winogradow, A. and Pempkowiak, J.: Organic carbon burial rates in the Baltic Sea sediments, Estuar. Coast. Shelf S., 138, 27–36, doi:10.1016/j.ecss.2013.12.001, 2014.

Winterwerp, J. C., van Kesteren, W. G. M., van Prooijen, B., and Jacobs, W.: A conceptual framework for shear flow–induced erosion of soft cohesive sediment beds, J. Geophys. Res. Oceans, 117, doi:10.1029/2012JC008072, 2012.

Xiao, K., Chen, N., Wang, Z. A., Tamborski, J. J., Maher, D. T., and Yu, X.: Editorial: Advances in understanding lateral blue carbon export from coastal ecosystems, Front. Mar. Sci., 9, 2022.

Zhang, Y. J., Ye, F., Stanev, E. V., and Grashorn, S.: Seamless cross-scale modeling with SCHISM, Ocean Model., 102, 64–81, doi:10.1016/j.ocemod.2016.05.002, 2016.

Zhao, C., Daewel, U., and Schrum, C.: Tidal impacts on primary production in the North Sea, Earth Syst. Dynam., 10, 287–317, doi:10.5194/esd-10-287-2019, 2019.